Estimates for the single-spin asymmetries in $p^{\uparrow}p \to J/\psi X$ process at PHENIX RHIC and SPD NICA

A. V. Karpishkov[1,2], M. A. Nefedov[1], and V. A. Saleev[1,2]

[1] Samara National Research University
[2] Joint Institute for Nuclear Research

30.09.2020
Gluon content of proton and deuteron with the Spin Physics Detector at the NICA collider

Outline

1. Generalized Parton Model (GPM)
   - Factorization formula for the GPM
   - Trento convention for TSSA
2. **Models of J/ψ production: NRQCD versus ICEM**
   - NRQCD approach
   - ICEM approach
3. TSSA in charmonium production at RHIC and NICA
   - Comparison to PHENIX RHIC data
   - **Predictions for SPD NICA**
4. Conclusions

The "incomplete" list of relevant recent articles

- U. D'Alesio, C. Flore, F. Murgia, C. Pisano and P. Taels, "Unraveling the Gluon Sivers Function in Hadronic Collisions at RHIC," Phys. Rev. D **99**, no.3, 036013 (2019)
- U. D' Alesio, L. Maxia, F. Murgia, C. Pisano and S. Rajesh, "Process dependence of the gluon Sivers function in $p^{\uparrow}p \to J/\psi + X$ within a TMD approach in NRQCD," [arXiv:2007.03353 [hep-ph]].
- U. D'Alesio, F. Murgia, C. Pisano and S. Rajesh, "Single-spin asymmetries in $p^{\uparrow}p \to J/\psi + X$ within a TMD approach: role of the color octet mechanism," Eur. Phys. J. C **79**, no.12, 1029 (2019)
- U. D'Alesio, F. Murgia, C. Pisano and P. Taels, "Probing the gluon Sivers function in $p^{\uparrow}p \to J/\psi\, X$ and $p^{\uparrow}p \to D\, X$," Phys. Rev. D **96**, no.3, 036011 (2017)
- R. M. Godbole, A. Kaushik, A. Misra, V. Rawoot and B. Sonawane, "Transverse single spin asymmetry in $p + p^{\uparrow} \to J/\psi + X$," Phys. Rev. D **96**, no.9, 096025 (2017)

Generalized Parton Model (GPM)

Factorization schemes

The Collinear Parton Model (CPM) is applicable in a region of high-p_T production

$$p_T \gg 1\text{GeV},$$

so we can neglect small intrinsic $\mathbf{q_T}$ of initial partons ($\langle q_T^2 \rangle \simeq 1$ GeV^2).

If we're interested in particle production in a region of $p_T \simeq \sqrt{\langle q_T^2 \rangle} \ll \mu_F \simeq m_{J/\psi}$, we should take into account intrinsic q_T within TMD approach, [J. Collins, Camb. Monogr., Part. Phys. Nucl. Phys. Cosmol. 32, 1-624 (2011)].

Here we use phenomenological TMD-based approach, Generalized Parton Model (GPM), where simple prescription for TMD parton distribution functions (PDFs) is used:

$$F_a(x, q_T, \mu_F) = f_a(x, \mu_F) \times G_a(q_T), \tag{1}$$

where $f_a(x, \mu_F)$ – corresponding collinear PDF, $G_a(q_T)$ – Gaussian distribution

$$G_a(q_T) = \exp(-q_T^2/\langle q_T^2 \rangle_a)/(\pi \langle q_T^2 \rangle_a)$$

.

Factorization formula for the GPM

Within the GPM we can write the differential cross-section as follows

$$d\sigma(pp \to \mathcal{C}X) = \int dx_1 \int d^2\mathbf{q_{1T}} \int dx_2 \int d^2\mathbf{q_{2T}} \times$$
$$\times F_g(x_1, q_{1T}, \mu_F) F_g(x_2, q_{2T}, \mu_F) d\hat{\sigma}(gg \to \mathcal{C}), \quad (2)$$

where $\mathcal{C} = J/\psi, \psi(2S)$ or $\chi_c(1P)$.
For $2 \to 1$ hard subprocess $g(q_1) + g(q_2) \to \mathcal{C}(k)$:

$$d\hat{\sigma}(gg \to \mathcal{C}) = (2\pi)^4 \delta^{(4)}(q_1 + q_2 - k) \frac{\overline{|M(gg \to \mathcal{C})|^2}}{2x_1 x_2 s} \frac{d^4k}{(2\pi)^3} \delta_+(k^2 - m_{\mathcal{C}}^2). \quad (3)$$

In a case of $2 \to 2$ subprocess $g(q_1) + g(q_2) \to \mathcal{C}(k) + g(q_3)$, $\mathcal{C} = J/\psi, \psi(2S)$:

$$d\hat{\sigma}(gg \to \mathcal{C}g) = (2\pi)^4 \delta^{(4)}(q_1 + q_2 - k - q_3) \frac{\overline{|M(gg \to \mathcal{C}g)|^2}}{2x_1 x_2 s} \frac{d^3k}{(2\pi)^3 2k_0} \frac{d^4 q_3}{(2\pi)^3} \delta_+(q_3^2). \quad (4)$$

Transverse Single Spin Asymmetry

In inclusive process $p^{\uparrow}p \to \mathcal{C}X$ $\mathcal{C} = J/\psi, \chi_c, \psi(2S))$ TSSA is defined as:

$$A_N = \frac{d\sigma^{\uparrow} - d\sigma^{\downarrow}}{d\sigma^{\uparrow} + d\sigma^{\downarrow}} = \frac{d\Delta\sigma}{2d\sigma}. \tag{5}$$

The numerator and denominator of A_N have the form:

$$d\sigma \propto \int dx_1 \int d^2q_{1T} \int dx_2 \int d^2q_{2T} F_g(x_1, q_{1T}, \mu_F) F_g(x_2, q_{2T}, \mu_F) d\hat{\sigma}(gg \to \mathcal{C}X), \tag{6}$$

$$d\Delta\sigma \propto \int dx_1 \int d^2q_{1T} \int dx_2 \int d^2q_{2T} [\hat{F}_g^{\uparrow}(x_1, \mathbf{q}_{1T}, \mu_F) - \hat{F}_g^{\downarrow}(x_1, \mathbf{q}_{1T}, \mu_F)] \times F_g(x_2, q_{2T}, \mu_F) d\hat{\sigma}(gg \to \mathcal{C}X), \tag{7}$$

where $\hat{F}_g^{\uparrow,\downarrow}(x, q_T, \mu_F)$ is the distribution of unpolarized gluon (or quark) in polarized proton.
Following the Trento conventions [A. Bacchetta, U. D'Alesio, M. Diehl and C. A. Miller, Phys. Rev. D **70**, 117504 (2004)], the gluon Sivers function (GSF) can be introduced as

$$\begin{aligned} \Delta\hat{F}_g^{\uparrow}(x_1, \mathbf{q}_{1T}, \mu_F) &\equiv \hat{F}_g^{(\uparrow)}(x_1, \mathbf{q}_{1T}, \mu_F) - \hat{F}_g^{(\downarrow)}(x_1, \mathbf{q}_{1T}, \mu_F) \\ &= \Delta^N F_g^{\uparrow}(x_1, \mathbf{q}_{1T}^2, \mu_F) \cos(\phi_1). \end{aligned} \tag{8}$$

Parameterizationa for GSF

Gluon Sivers function may be presented in the form

$$\Delta^N F_g^{\uparrow}(x, q_T^2, \mu_F) = 2\frac{\sqrt{2e}}{\pi} N_g(x) f_g(x, \mu_F) \sqrt{\frac{1-\rho_g}{\rho_g}} \frac{q_T}{\langle q_T^2 \rangle_g^{3/2}} e^{-q_T^2/\rho_g \langle q_T^2 \rangle_g}. \qquad (9)$$

GSF set	N_g	α_g	β_g	ρ_g	$\langle q_T^2 \rangle_g$, GeV^2
SIDIS1	0.65	2.8	2.8	0.687	0.25
SIDIS2	0.05	0.8	1.4	0.576	0.25
D'Alesio *et al.*	0.25	0.6	0.6	0.1	1.0

Table: Parameters of GSFs

Models of J/ψ production: NRQCD and ICEM

Basics of NRQCD factorization

The NRQCD framework [G. T. Bodwin, E. Braaten, and G. P. Lepage, Phys. Rev. D **51**, 1125 (1995)] describes heavy quarkonium in terms of Fock state decomposition:

$$|\mathcal{H}\rangle = \mathcal{O}(v^0)|Q\bar{Q}[^3S_1^{(1)}]\rangle + \mathcal{O}(v)|Q\bar{Q}[^3P_J^{(8)}]g\rangle + \mathcal{O}(v^2)|Q\bar{Q}[^1S_0^{(8)}]g\rangle \quad (10)$$

$$+\mathcal{O}(v^2)|Q\bar{Q}[^3S_1^{(1,8)}]gg\rangle + \dots \quad (11)$$

In the NRQCD effects of short and long distances are separated, and cross-section of heavy-quarkonium production via a partonic subprocess $a + b \to \mathcal{H} + X$ can be presented in a factorized form:

$$d\hat{\sigma}(a + b \to \mathcal{H} + X) = \sum_n d\hat{\sigma}(a + b \to Q\bar{Q}[n] + X) \times \langle\mathcal{O}^{\mathcal{H}}[n]\rangle, \quad (12)$$

where n denotes the set of quantum numbers of the $Q\bar{Q}$ pair, and its transitions into $\mathcal{H}$ is described by the Long-Distance Matrix Elements (LDMEs) $\langle\mathcal{O}^{\mathcal{H}}[n]\rangle$. The partonic cross-section of quarkonium production from the $Q\bar{Q}$ Fock state $n =^{2S+1} L_J^{(1,8)}$ has the form:

$$d\hat{\sigma}(a + b \to Q\bar{Q}[^{2S+1}L_J^{(1,8)}] \to \mathcal{H}) = d\hat{\sigma}(a + b \to Q\bar{Q}[^{2S+1}L_J^{(1,8)}]) \times \frac{\langle\mathcal{O}^{\mathcal{H}}[^{2S+1}L_J^{(1,8)}]\rangle}{N_{col}N_{pol}},$$

where $N_{col} = 2N_c$ for color-singlet state, $N_{col} = N_c^2 - 1$ for color-octet state, and $N_{pol} = 2J + 1$.

Amplitude of specified state

The definition of partonic cross-section of $Q\bar{Q}[^{2S+1}L_J^{(1,8)}]$ production is following:

$$d\hat{\sigma}(a+b \to Q\bar{Q}[^{2S+1}L_J^{(1,8)}]) = \frac{1}{2x_1x_2S}\overline{|\mathcal{A}(a+b \to Q\bar{Q}[^{2S+1}L_J^{(1,8)}])|^2}d\Phi. \qquad (13)$$

The projectors on spin-zero and spin-one states:

$$\Pi_0 = \frac{1}{8m^3}\left(\frac{\hat{p}}{2} - \hat{q} - m\right)\gamma^5\left(\frac{\hat{p}}{2} + \hat{q} + m\right), \Pi_1^\alpha = \frac{1}{8m^3}\left(\frac{\hat{p}}{2} - \hat{q} - m\right)\gamma^\alpha\left(\frac{\hat{p}}{2} + \hat{q} + m\right).$$

The projectors on color-singlet and color-octet states:

$$C_1 = \frac{\delta_{ij}}{\sqrt{N_c}}, \; C_8 = \sqrt{2}T^a_{ij},$$

respectively, where T^a with $a = 1, \cdots, N_c^2 - 1$ are the generators of the color gauge group $SU(N_c)$.

Long-distance matrix elements

We adopt the following values of color-singlet LDMEs
Color-singlet LDMEs can be determined from measured decay widths of charmonia using the known next-to-leading-order (NLO) QCD result or from calculations in potential models:
$\langle \mathcal{O}^{J/\psi}[^3S_1^{(1)}] \rangle = 1.3\ \mathrm{GeV}^3$,
$\langle \mathcal{O}^{\psi'}[^3S_1^{(1)}] \rangle = 6.5 \times 10^{-1}\ \mathrm{GeV}^3$
$\langle \mathcal{O}^{\chi_{cJ}}[^3P_J^{(1)}] \rangle = (2J+1) \times 8.9 \times 10^{-2}\ \mathrm{GeV}^5$.

Color-octet LDMEs should be universal and process-independent parameters. However, their numerical values strongly depend on approach which is used to describe $c\bar{c}-$pair production and data included into the fit.
Nevertheless, the hierarchy expected from velocity-scaling rules is respected by all the fits:

$$\langle \mathcal{O}^{\mathcal{C}}[^3P_0^{(1)}] \rangle \gg \langle \mathcal{O}^{\mathcal{C}}[^3P_0^{(8)}] \rangle$$

,

$$\langle \mathcal{O}^{\mathcal{C}}[^3S_1^{(1)}] \rangle \gg \langle \mathcal{O}^{\mathcal{C}}[^3P_J^{(8)}] \rangle \gg \left(\langle \mathcal{O}^{\mathcal{C}}[^3S_1^{(8)}] \rangle, \langle \mathcal{O}^{\mathcal{C}}[^1S_0^{(8)}] \rangle \right)$$

.

Short-distance coefficients

Squared LO in α_S amplitudes for $2 \to 1$ subprocesses in CPM are well-known [P.L. Cho, A.K. Leibovich (1996)]:

$$\overline{|\mathcal{A}(g+g\to\chi_{c0}[^3P_0^{(1)}]|^2} = \frac{8}{3}\pi^2\alpha_s^2\frac{\langle\mathcal{O}^{\chi_{c0}}[^3P_0^{(1)}]\rangle}{M^3}, \tag{14}$$

$$\overline{|\mathcal{A}(g+g\to\chi_{c1}[^3P_1^{(1)}]|^2} = 0, \tag{15}$$

$$\overline{|\mathcal{A}(g+g\to\chi_{c2}[^3P_2^{(1)}]|^2} = \frac{32}{45}\pi^2\alpha_s^2\frac{\langle\mathcal{O}^{\chi_{c2}}[^3P_2^{(1)}]\rangle}{M^3}, \tag{16}$$

$$\overline{|\mathcal{A}(g+g\to\mathcal{C}[^3S_1^{(8)}]|^2} = 0, \tag{17}$$

$$\overline{|\mathcal{A}(g+g\to\mathcal{C}[^1S_0^{(8)}]|^2} = \frac{5}{12}\pi^2\alpha_s^2\frac{\langle\mathcal{O}^{\mathcal{C}}[^1S_0^{(8)}]\rangle}{M}, \tag{18}$$

$$\overline{|\mathcal{A}(g+g\to\mathcal{C}[^3P_0^{(8)}]|^2} = 5\pi^2\alpha_s^2\frac{\langle\mathcal{O}^{\mathcal{C}}[^3P_0^{(8)}]\rangle}{M^3}, \tag{19}$$

$$\overline{|\mathcal{A}(g+g\to\mathcal{C}[^3P_1^{(8)}]|^2} = 0, \tag{20}$$

$$\overline{|\mathcal{A}(g+g\to\mathcal{C}[^3P_2^{(8)}]|^2} = \frac{4}{3}\pi^2\alpha_s^2\frac{\langle\mathcal{O}^{\mathcal{C}}[^3P_2^{(8)}]\rangle}{M^3}, \tag{21}$$

$$\overline{|\mathcal{A}(q+\bar{q}\to\mathcal{C}[^3S_1^{(8)}]|^2} = \frac{16}{27}\pi^2\alpha_s^2\frac{\langle\mathcal{O}^{\mathcal{C}}[^3S_1^{(8)}]\rangle}{M}. \tag{22}$$

Short-distance coefficients

The leading α_S $2 \to 2$ partonic subprocess, which describes direct production of J/ψ or $\psi(2S)$ via color-singlet intermediate state $[{}^3S_1^{(1)}]$, is $g + g \to \mathcal{C}[{}^3S_1^{(1)}] + g$. The squared amplitude for this partonic subprocess reads [R. Gastmans, W. Troost and T. T. Wu, Phys. Lett. B **184**, 257-260 (1987)]:

$$\overline{|\mathcal{A}(g + g \to \mathcal{C}[{}^3S_1^{(1)}] + g|^2} = \pi^3 \alpha_s^3 \frac{\langle \mathcal{O}^{\mathcal{C}}[{}^3S_1^{(1)}] \rangle}{M^3} \frac{320 M^4}{81(M^2 - \hat{t})^2 (M^2 - \hat{u})^2 (\hat{t} + \hat{u})^2} \times$$
$$\times (M^4 \hat{t}^2 - 2M^2 \hat{t}^3 + \hat{t}^4 + M^4 \hat{t}\hat{u} - 3M^2 \hat{t}^2 \hat{u} + 2\hat{t}^3 \hat{u} + M^4 \hat{u}^2 -$$
$$- 3M^2 \hat{t}\hat{u}^2 + 3\hat{t}^2 \hat{u}^2 - 2M^2 \hat{u}^3 + 2\hat{t}\hat{u}^3 + \hat{u}^4). \quad (23)$$

Improved Color Evaporation Model (ICEM)

In the ICEM [Y.Q. Ma and R. Vogt, Phys. Rev. D **94** (2016) 114029], it is assumed that all $c\bar{c}$ pairs with invariant masses below the $D\bar{D}$-threshold hadronize to charmonia with some probability, which is independent from angular momentum and spin quantum numbers of the pair:

$$\frac{d\sigma^{\mathcal{C}}}{d^3k} = F_{\mathcal{C}} \times \int_{m_C^2}^{4m_D^2} dM_{c\bar{c}}^2 \frac{d\sigma^{c\bar{c}}}{dM_{c\bar{c}}^2 d^3k}, \tag{24}$$

where $F_{\mathcal{C}}$ is the process-independent hadronization probability to the charmonium state $\mathcal{C}$.

Cross section of the ICEM

Cross section in GPM and ICEM reads:

$$\begin{aligned} \frac{d\sigma^{\mathcal{C}}}{d^3k} &= F_{\mathcal{C}} \times \int dx_1 \int d^2 q_{1T} \int dx_2 \; F_g(x_1, q_{1T}, \mu_F) F_g(x_2, q_{2T}, \mu_F) \hat{\sigma}(\hat{s}, ij \to c\bar{c}) \\ &\times \delta(q_1^3 + q_2^3 - k^3) \left[\theta(\hat{s} - m_{\mathcal{C}}^2) - \theta(\hat{s} - 4m_D^2)\right], \end{aligned} \tag{25}$$

where $\hat{\sigma}(\hat{s}, ij \to c\bar{c})$ is just a well-known total cross section of one of the subprocesses: $gg \to c\bar{c}$ or $q\bar{q} \to c\bar{c}$, correspondingly.

TSSA in charmonium production at RHIC and NICA

PHENIX-2012 data, $|y| \leq 0.35$, $\sqrt{S} = 200$ GeV.

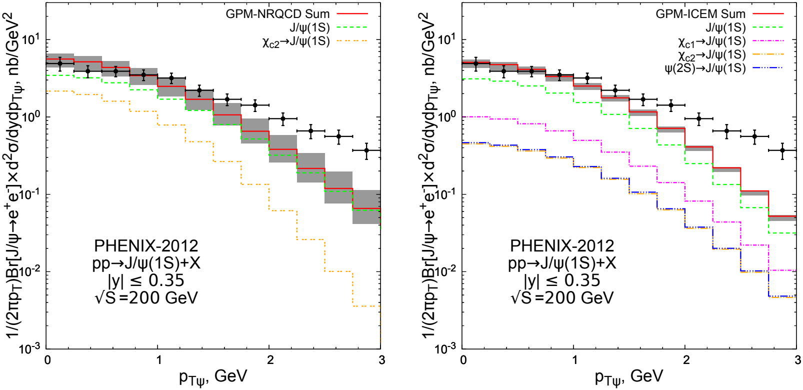

Figure: Differential cross-section of prompt J/ψ production as function of transverse momentum at $\sqrt{s} = 200$ GeV, $|y| \leq 0.35$. The theoretical results are obtained in GPM with $\langle q_T^2 \rangle = 1$ GeV^2. Left panel: NRQCD-factorization prediction with only color-singlet channels included. Right panel: ICEM-prediction. In the left panel, contributions from decays $\chi_{c0} \to J/\psi$ and $\psi(2S) \to J/\psi$ are not shown. Experimental data are from the Ref. [A. Adare *et al.* [PHENIX], Phys. Rev. D **85**, 092004 (2012)].

PHENIX-2012 data, $|y| \leq 0.35$, $\sqrt{S} = 200$ GeV.

Table: The relative contributions of direct and feed-down production within NRQCD and ICEM. Experimental data of the PHENIX collaboration for $\sqrt{s} = 200$ GeV are from [A. Adare *et al.* [PHENIX], Phys. Rev. D **85**, 092004 (2012)].

$\sqrt{s}$	Model/Source of data	$\sigma^{\text{direct}} : \sigma^{\chi_c \to J/\psi} : \sigma^{\psi(2S)\to J/\psi}$
24 GeV	NRQCD	0.58 : 0.39 : 0.03
24 GeV	ICEM	0.68 : 0.25 : 0.07
200 GeV	NRQCD	0.61 : 0.34 : 0.05
200 GeV	ICEM	0.61 : 0.30 : 0.09
200 GeV	PHENIX collab.	0.58 : 0.32 : 0.10

Table: The values of hadronization probabilities of ICEM, which had been obtained via the fit of total cross-section of J/ψ-production at PHENIX. The fit of LHC data are taken from [V. Cheung and R. Vogt, Phys. Rev. D **98**, 114029 (2018)].

$F_{\mathcal{C}}$	Our fit	The fit of LHC data
$F_{J/\psi}$	0.02	0.02
$F_{\chi_{c1}}$	0.06	0.18
$F_{\chi_{c2}}$	0.06	0.2
$F_{\psi'}$	0.08	0.12

PHENIX-2018 data, $1.2 \leq |y| \leq 2.2$, $\sqrt{S} = 200$ GeV.

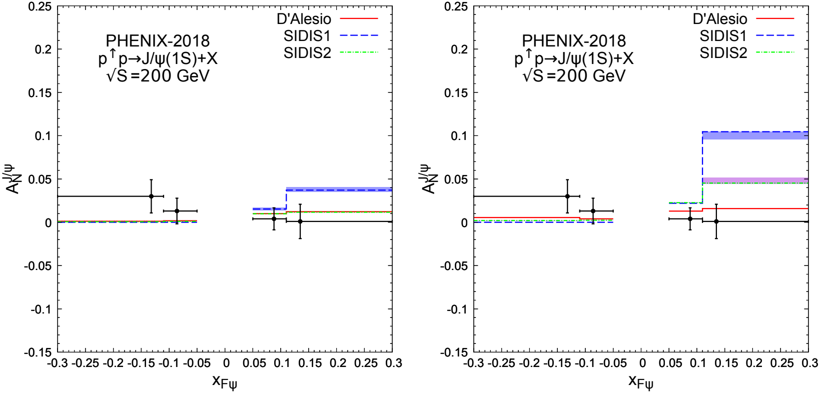

Figure: SSA $A_N^{J/\psi}$ as function of x_F at $\sqrt{s} = 200$ GeV. The theoretical results are obtained with SIDIS1 and D'Alesio *et al.* parameterizations of GSFs. Experimental data are from Ref. [C. Aidala *et al.* [PHENIX], Phys. Rev. D **98**, 012006 (2018)]. Left panel: NRQCD-prediction. Right panel: ICEM prediction.

PHENIX-2018 data, $1.2 \leq |y| \leq 2.2$, $\sqrt{S} = 200$ GeV.

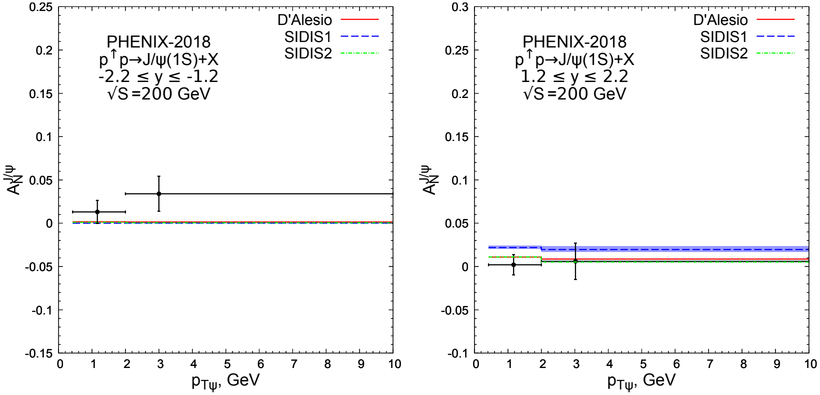

Figure: NRQCD predictions for SSA $A_N^{J/\psi}$ as function of J/ψ-transverse momentum at $\sqrt{s} = 200$ GeV. The theoretical results are obtained with SIDIS1 and D'Alesio et al. parameterizations of GSFs. Left panel – backward production ($-2.2 \leq y \leq -1.2$), right panel – forward production ($1.2 \leq y \leq 2.2$). Experimental data are from Ref. [C. Aidala *et al.* [PHENIX], Phys. Rev. D **98**, 012006 (2018)].

PHENIX-2018 data, $1.2 \leq |y| \leq 2.2$, $\sqrt{S} = 200$ GeV.

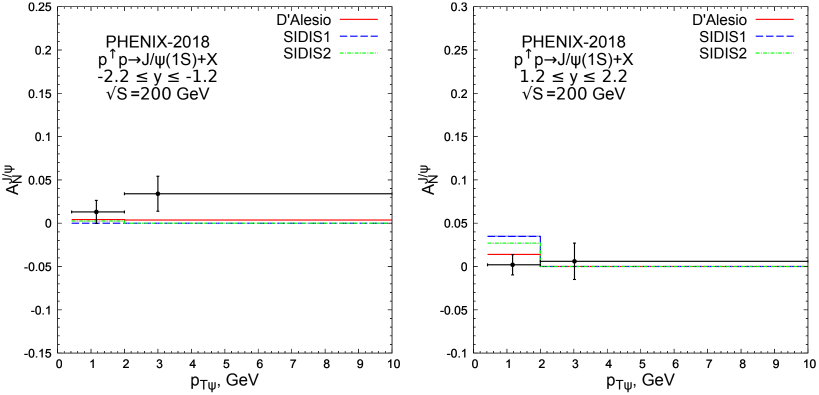

Figure: ICEM predictions for SSA $A_N^{J/\psi}$ as function of J/ψ-transverse momentum at $\sqrt{s} = 200$ GeV. The theoretical results are obtained with SIDIS1 and D'Alesio et al. parameterizations of GSFs. Left panel – backward production ($-2.2 \leq y \leq -1.2$), right panel – forward production ($1.2 \leq y \leq 2.2$). Experimental data are from Ref. [C. Aidala *et al.* [PHENIX], Phys. Rev. D **98**, 012006 (2018)].

Predictions for TSSA in J/ψ production at PHENIX , $\sqrt{S} = 200$ GeV.

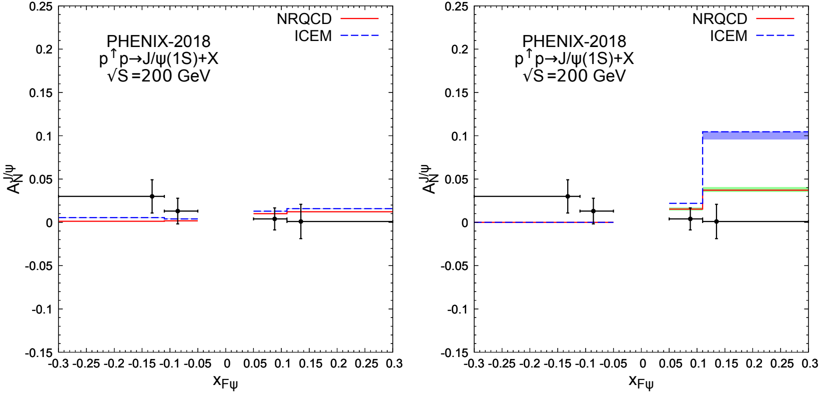

Figure: Comparison of predictions for SSA $A_N^{J/\psi}$ as function of x_F with the D'Alesio *et al.* parameterization of GSF (left panel) and SIDIS1 (right panel) at $\sqrt{s} = 24$ GeV in NRQCD (solid histogram) and ICEM (dashed histogram) approaches. s is used.

Predictions for NICA (in different models), $|y| \leq 3$, $\sqrt{S} = 24$ GeV.

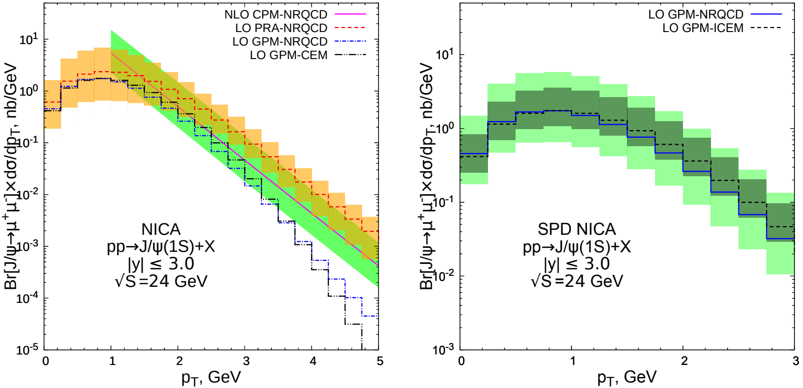

Figure: Prompt J/ψ transverse momentum distribution at $\sqrt{s} = 24$ GeV, $|y| \leq 3$. Left panel: GPM results with $\langle q_T^2 \rangle = 1$ GeV^2 are shown by dash-dotted (NRQCD) and dash-double-dotted (ICEM) histograms. Solid and dashed histograms with uncertainty bands are PRA [A.V. Karpishkov, M.A. Nefedov and V.A. Saleev, J. Phys. Conf. Ser. **1435**, 012015 (2020)] and NLO CPM [M. Butenschön and B.A. Kniehl, private communication] predictions respectively. Right panel: GPM predictions in NRQCD (solid histogram with light green uncertainty band) and ICEM (dashed histogram with dark-green uncertainty band) approaches with their uncertainty bands shown.

Predictions for SSA at NICA (SIDIS1), $|y| \leq 3$, $\sqrt{S} = 24$ GeV.

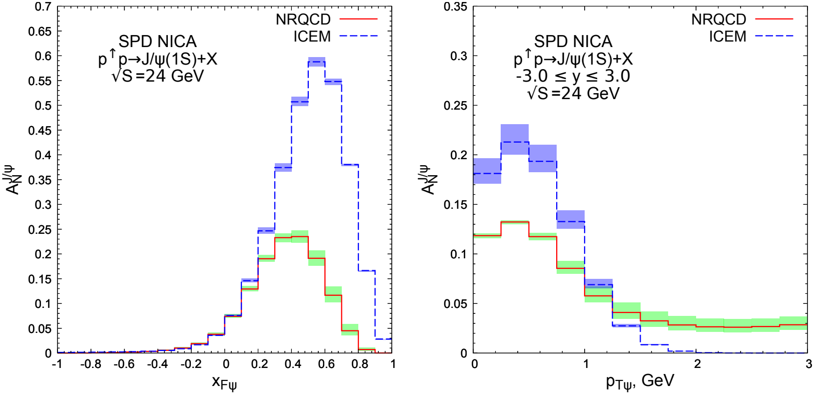

Figure: Comparison of predictions for SSA $A_N^{J/\psi}$ as function of x_F (left panel) and transverse momentum (right panel) at $\sqrt{s} = 24$ GeV in NRQCD (solid histogram) and ICEM (dashed histogram) approaches. The SIDIS1 parametrisation of GSFs is used.

Predictions for TSSA at NICA (D'Alesio), $|y| \leq 3$, $\sqrt{S} = 24$ GeV.

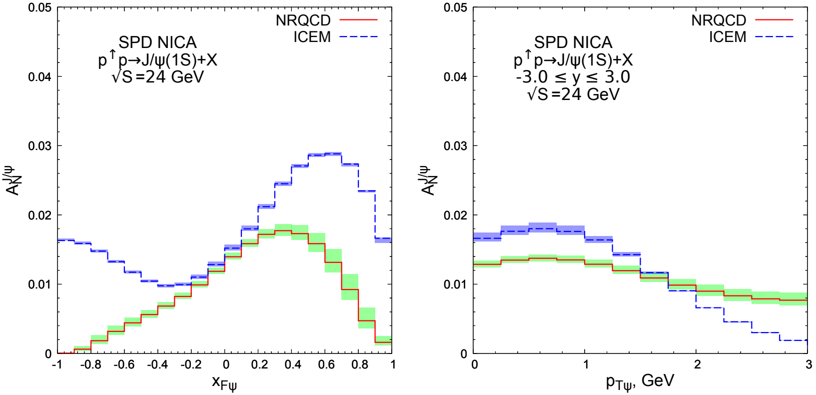

Figure: Comparison of predictions for SSA $A_N^{J/\psi}$ as function of x_F (left panel) and transverse momentum (right panel) at $\sqrt{s} = 24$ GeV in NRQCD (solid histogram) and ICEM (dashed histogram) approaches. The D'Alesio *et al.* parametrisation of GSFs is used.

Predictions for TSSA in χ_{c2} production at NICA , $|y| \leq 3$, $\sqrt{S} = 24$ GeV.

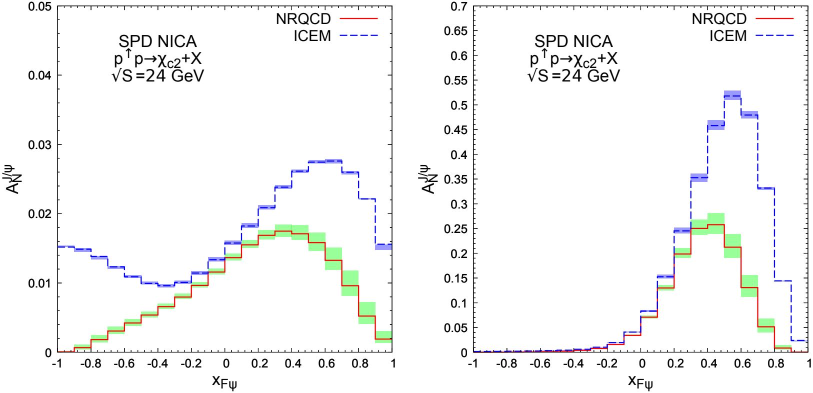

Figure: Comparison of predictions for SSA $A_N^{\chi_{c2}}$ as function of x_F with the D'Alesio *et al.* parameterization of GSF (left panel) and SIDIS1 (right panel) at $\sqrt{s} = 24$ GeV in NRQCD (solid histogram) and ICEM (dashed histogram) approaches. s is used.

Conclusions

- Prompt J/ψ transverse momentum spectra at small $k_{T\,J/\psi} < m_{J/\psi}$ can be described well in GPM, as in the Color Singlet Model of NRQCD, as in the ICEM. The total cross-section ratios of direct and feed-down contributions in good agreement with experimental data too.
- We find, that parametrization of D'Alesio *et al.* for GSF leads to reasonable predictions for magnitude, J/ψ transverse momentum and x_F dependence of the TSSA at PHENIX RICH.
- We demonstrate measurable differences in predictions of TSSAs obtained in NRQCD versus ICEM, especially at SPD NICA experiment.
- The predictions for TSSAs at the planned SPD NICA experiment are presented for the first time.

For details, see [A.V. Karpishkov, M.A. Nefedov, V.A. Saleev, arXiv:2008.07232].

Thank you for your attention!